

Topological Insulators with SU(2) Landau Levels

Yi Li,^{1,2} Shou-Cheng Zhang,³ and Congjun Wu¹

¹*Department of Physics, University of California, San Diego, La Jolla, California 92093, USA*

²*Princeton Center for Theoretical Science, Princeton University, Princeton, New Jersey 08544, USA*

³*Department of Physics, Stanford University, Stanford, California 94305, USA*

(Received 14 August 2012; revised manuscript received 3 June 2013; published 30 October 2013)

We construct continuum models of 3D and 4D topological insulators by coupling spin- $\frac{1}{2}$ fermions to an SU(2) background gauge field, which is equivalent to a spatially dependent spin-orbit coupling. Higher dimensional generalizations of flat Landau levels are obtained in the Landau-like gauge. The 2D helical Dirac modes with opposite helicities and 3D Weyl modes with opposite chiralities are spatially separated along the third and fourth dimensions, respectively. Stable 2D helical Fermi surfaces and 3D chiral Fermi surfaces appear on open boundaries, respectively. The charge pumping in 4D Landau level systems shows quantized 4D quantum Hall effect.

DOI: [10.1103/PhysRevLett.111.186803](https://doi.org/10.1103/PhysRevLett.111.186803)

PACS numbers: 73.43.Cd, 71.70.Ej, 73.21.-b

Time-reversal (TR) invariant topological insulators (TIs) have become a major research focus in condensed matter physics [1–3]. Different from the 2D quantum Hall (QH) and quantum anomalous Hall systems which are topologically characterized by the first Chern number [4–8], time-reversal invariant TIs are characterized by the second Chern number in 4D [9,10] and the \mathbb{Z}_2 index in 2D and 3D [10–16]. Various 2D and 3D TIs are predicted theoretically and identified experimentally exhibiting stable gapless 1D helical edge and 2D surface modes against TR invariant perturbations [13,17–21]. Topological states have also been extended to systems with particle-hole symmetry and superconductors [22–24].

Most current studies of 2D and 3D TIs focus on Bloch-wave bands in lattice systems. The nontrivial band topology arises from spin-orbit (SO) coupling induced band inversions [13]. However, Landau levels (LL) are essential in the study of QH effects because their elegant analytical properties enable construction of fractional states. Generalizing LLs to high dimensions gives rise to TIs with explicit wave functions in the continuum, which would facilitate the study of the exotic fractional TIs. Efforts along this line were pioneered by Zhang and Hu [9]. They constructed LLs on the compact S^4 sphere by coupling fermions with the SU(2) monopole gauge potential, and various further developments appeared [25–29]. Two dimensional TIs based on TR invariant LLs have also been investigated [12]. Two of the authors generalized LLs of Schrödinger fermions to high-dimensional flat space [30] by combining the isotropic harmonic potential and SO coupling. LLs have also been generalized to high dimensional Dirac fermions and parity-breaking systems [31,32].

In all the above works, angular momentum is explicitly conserved; thus, they can be considered as LLs in the symmetriclike gauge. In 2D, LL wave functions in the Landau gauge are particularly intuitive: they are 1D chiral

plane wave modes spatially separated along the transverse direction. The QH effect is just the 1D chiral anomaly in which the chiral current generated by the electric field becomes the transverse charge current. In this Letter, we develop high dimensional LLs with flat spectra as spatially separated helical Dirac or chiral Weyl fermion modes, i.e., the SU(2) Landau-like gauge. They are 3D and 4D TIs defined in the continuum possessing stable gapless boundary modes. To our knowledge, these are the simplest TI Hamiltonians constructed so far. Recently, there have been considerable interests of 2D topological band structures with approximate flat spectra [33–35]. Our Hamiltonians defined in the continuum possess exact flat energy spectra in 3D and 4D, and are independent of the band inversion mechanism. For the 4D case, they exhibit the 4D quantum Hall effect [9,10], which is a quantized nonlinear electromagnetic response related to the spatially separated (3 + 1)D chiral anomaly. Our methods can be easily generalized to arbitrary dimensions and also to Dirac fermions.

The 3D case.—We begin with the 3D TR invariant LL Hamiltonian for a spin- $\frac{1}{2}$ fermion as

$$H_{LL}^{3D} = \frac{\vec{p}^2}{2m} + \frac{1}{2}m\omega_{so}^2z^2 - \omega_{so}z(p_x\sigma_y - p_y\sigma_x), \quad (1)$$

which couples the 1D harmonic potential in the z direction and the 2D Rashba SO coupling through a z -dependent SO coupling strength. H_{LL}^{3D} possess translation symmetry in the xy plane, TR and parity symmetries. Equation (1) can be reformulated in the form of an SU(2) background gauge potential as $H_{LL}^{3D} = (1/2m)(\vec{p} - \frac{e}{c}\vec{A})^2 - \frac{1}{2}m\omega_{so}^2z^2$, where $\omega_{so} = |eG|/mc$, and \vec{A} takes the Landau-like gauge as $A_x = G\sigma_yz$, $A_y = -G\sigma_xz$, and $A_z = 0$. In Ref. [30], a symmetriclike gauge with $\vec{A}' = G\vec{\sigma} \times \vec{r}$ is used, which explicitly preserves the 3D rotational symmetry. However, the SU(2) vector potentials \vec{A}' and \vec{A} are *not* gauge equivalent. As shown below, the physical quantities

of Eq. (1), such as density of states, are not 3D rotationally symmetric. Nevertheless, we will see below that these two Hamiltonians give rise to the same forms of helical Dirac surface modes, and thus they belong to the same topological class. A related Hamiltonian is also employed for studying electromagnetic properties in superconductors with cylindrical geometry [36].

Equation (1) can be decomposed into a set of 1D harmonic oscillators along the z axis exhibiting flat spectra, a key feature of LLs. We define a characteristic SO length scale $l_{so} = \sqrt{\hbar/(m\omega_{so})}$. Each of the reduced 1D harmonic oscillator Hamiltonian is associated with a 2D helical plane wave state as $H^z(\vec{k}_{2D}) = (p_z^2/2m) + \frac{1}{2}m\omega_{so}^2[z - l_{so}^2 k_{2D} \hat{\Sigma}_{2D}(\hat{k}_{2D})]^2$, where $k_{2D} = (k_x^2 + k_y^2)^{1/2}$ and $\vec{k}_{2D} = (k_x, k_y)$; the helicity operator is defined as $\hat{\Sigma}_{2D}(\hat{k}_{2D}) = \hat{k}_x \sigma_y - \hat{k}_y \sigma_x$. The n -th LL eigenstates are solved as

$$\Psi_{n, \vec{k}_{2D}, \Sigma}(\vec{r}) = e^{i\vec{k}_{2D} \cdot \vec{r}_{2D}} \phi_n[z - z_0(k_{2D}, \Sigma)] \otimes \chi_{\Sigma}(\hat{k}_{2D}), \quad (2)$$

where $\vec{r}_{2D} = (x, y)$; $\chi_{\Sigma}(\hat{k}_{2D})$ are eigenstates of the helicity satisfying $\hat{\Sigma}_{\Sigma}(\hat{k}_{2D}) = \Sigma \chi_{\Sigma}(\hat{k}_{2D})$ with helicity eigenvalues $\Sigma = \pm 1$; $\phi_n[z - z_0]$ are the eigenstates of the n -th harmonic levels with the central positions located at z_0 , and $z_0(k_{2D}, \Sigma) = \Sigma l_{so}^2 k_{2D}$. The energy spectra of the n -th LL is $E_n = (n + \frac{1}{2})\hbar\omega_{so}$, independent of \vec{k}_{2D} and Σ .

In the 2D LL case, spatial coordinates x and y are non-commutative if projected to a given LL, say, the lowest LL (LLL). The LLL wave functions in the Landau gauge are 1D plane waves along the x direction whose central y positions linearly depend on k_x as $y_0 = l_B^2 k_x$. These 1D modes with opposite chiralities are spatially separated along the y direction. Consequently, the xy plane can be viewed as the 2D phase space of a 1D system, in which y plays the role of k_x . The momentum cutoff of the bulk states is determined by the system size along the y direction as $|k_x| < (L_y/(2l_B^2))$. Right and left moving edge modes appear along the upper and lower boundaries perpendicular to the y axis, respectively. These chiral edge modes cannot exist in purely 1D systems such as quantum wires.

Similarly, the 3D LL wave functions in Eq. (2) are spatially separated 2D helical plane waves along the z axis. As shown in Fig. 1(a), for states with opposite helicity eigenvalues, their central positions are shifted in opposite directions. Let us perform the LLL projection. Among the LLL states with good quantum numbers (\vec{k}_{2D}, Σ) , it is easy to check the following matrix elements $\langle \Psi_{0, \vec{k}_{2D}, \Sigma} | z | \Psi_{0, \vec{k}'_{2D}, \Sigma'} \rangle = \delta(\vec{k}_{2D}, \vec{k}'_{2D}) \delta_{\Sigma, \Sigma'} z_0(k_{2D}, \Sigma)$. Therefore, we have $\langle \Psi_0^a | z | \Psi_0^b \rangle = \langle \Psi_0^a | (l_{so}^2/\hbar)(p_x \sigma_y - p_y \sigma_x) | \Psi_0^b \rangle$, where $\Psi_0^{a,b}$ are arbitrary linear superpositions of $\Psi_{0, \vec{k}_{2D}, \Sigma}$ in the LLL. This proves that

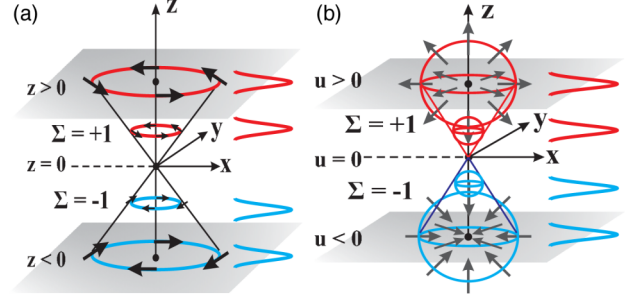


FIG. 1 (color online). 3D and 4D LLs for H_{LL}^{3D} and H_{LL}^{4D} as spatially separated 2D helical SO plane wave modes localized along the z axis (a), and 3D Weyl modes localized along the u axis (b), respectively. Their central locations are $z_0(\vec{k}_{2D}, \Sigma) = \Sigma l_{so}^2 k_{2D}$ and $u_0(\vec{k}_{3D}, \Sigma) = \Sigma l_{so}^2 k_{3D}$, respectively. Note that 2D Dirac modes with opposite helicities and the 3D ones with opposite chiralities are located at opposite sides of $z = 0$ and $u = 0$ planes, respectively.

$$PzP = \frac{l_{so}^2}{\hbar} (p_x \sigma_y - p_y \sigma_x), \quad (3)$$

where P is the LLL projection operator. Since the LLL states span the complete basis for the plane waves in the xy plane, the projections of x and y in the LLL remain themselves. As a result, we obtain the following commutation relations after the LLL projection as

$$[x, z]_{LLL} = il_{so}^2 \sigma_y, [y, z]_{LLL} = -il_{so}^2 \sigma_x, [x, y]_{LLL} = 0. \quad (4)$$

Interestingly, the 3D LL states can be viewed as states in the 4D phase space of a 2D system (with x and y coordinates) augmented by the helicity structure, in which $|z|$ plays the role of the magnitude of the 2D momentum and the sign of z corresponds to $\Sigma = \pm 1$. In fact, the momentum cutoff of the bulk states is exactly determined by the spatial size L_z along the z direction as

$$k_{2D} < k_{2D}^B \equiv \frac{L_z}{2l_{so}^2}, \quad (5)$$

in which $-(L_z/2) < z < (L_z/2)$. Applying the open boundary condition along the z direction and periodic boundary conditions in the x and y directions with spatial sizes L_x and L_y , respectively, we can easily count the total number of states to be $\mathcal{N} = L_x L_y L_z^2 / (8\pi l_{so}^4)$. The L_z^2 dependence of \mathcal{N} may seem puzzling for a 3D system, but expressing L_z in terms of Eq. (5), we find $\mathcal{N} = (1/2\pi) L_x L_y (k_{2D}^B)^2$, which is the conventional state counting of a 2D system expressed in terms of the 4D phase space volume. It means that an effectively 4D density of states are squeezed into a 3D real space.

The topological property of this 3D LL system manifests through its helical surface spectra. Let us consider the upper boundary located at $z = z_B$ for H_{LL}^{3D} . For simplicity, we only consider the LLL as an example. If $z_B > 0$, the positive helicity states $\Psi_{0, \vec{k}_{2D}, \Sigma=1}$ with $k_{2D} > k_{2D}^B = z_B l_{so}^{-2}$

are confined at the boundary. The 1D harmonic potential associated with \vec{k}_{2D} and $\Sigma = 1$ is truncated at $z = z_B$, and thus, the surface spectra acquire dispersion. If we neglect the zero-point energy, the surface mode dispersion is approximated by $\frac{1}{2}m\omega_{so}^2(k - k_{2D}^B)^2 l_{so}^4$ with $k > k_{2D}^B$. If the chemical potential μ lies above the LLL, it cuts the spectra at surface states with a Fermi wave vector $k_f > k_{2D}^B$. The Fermi velocity is $v_f \approx m(k_f - k_{2D}^B)\omega_{so}^2 l_{so}^4$. The surface Hamiltonian is approximated as $H_{sf} \approx v_f(\vec{p} \times \vec{\sigma}) \cdot \hat{z} - \mu$ with an electronlike Fermi surface with $\Sigma = 1$. In another case, if the upper boundary is located at $z_B < 0$, then the negative helicity states $\Psi_{0, \vec{k}_{2D}, \Sigma=-1}$ with $k_{2D} < k_{2D}^B$, and all the positive helicity states are pushed to the boundary as surface modes. Depending on the value of μ , we can have a holelike Fermi surface with $\Sigma = -1$, a Dirac Fermi point, or an electronlike Fermi surface with $\Sigma = 1$. Similarly, any other LL gives rise to a branch of gapless helical surface modes, and each filled bulk LL contributes one helical Fermi surface. For the lower boundary, the analysis is parallel to the above. Each filled LL gives rise to an electronlike helical Fermi surface with $\Sigma = -1$, or holelike with $\Sigma = 1$. According to the standard Z_2 classification, this system is topologically nontrivial if the Fermi energy cuts an odd number of Landau levels. So far, we have assumed the harmonic frequency and SO coupling frequency to be equal in Eq. (1). As explained in the Supplemental Material [37], although the equality of these two frequencies is essential for the spectra flatness, the \mathbb{Z}_2 topology does not require this equality.

The 4D case.—The above procedure can be straightforwardly generalized to any higher dimension. For example, the 4D LL Hamiltonian is denoted as

$$H_{LL}^{4D} = \frac{p_u^2}{2m} + \frac{1}{2}m\omega^2 u^2 + \frac{\vec{p}_{3D}^2}{2m} - \omega u \vec{p}_{3D} \cdot \vec{\sigma}, \quad (6)$$

where u and p_u refer to the coordinate and momentum of the 4th dimension, respectively, and \vec{p}_{3D} is the 3 momentum in the xyz space. Equation (6) can be represented as $H_{LL}^{4D} = (1/2m) \sum_{i=1}^4 (p_i - (e/c)A_i)^2 - m\omega^2 u^2$, where the SU(2) vector potential takes the Landau-like gauge with $A_i = G\sigma_i u$ for $i = x, y, z$ and $A_u = 0$. Equation (6) preserves the translational and rotational symmetries in the xyz space and TR symmetry. Similar to the 3D case, the 4D LL spectra and wave functions are solved by reducing Eq. (6) into a set of 1D harmonic oscillators along the u axis as $H^u(\vec{k}_{3D}) = (p_u^2/2m) + \frac{1}{2}m\omega^2(u - l_{so}^2 k_{3D} \hat{\Sigma}_{3D})^2$, where $k_{3D} = (k_x^2 + k_y^2 + k_z^2)^{1/2}$ and $\hat{\Sigma}_{3D} = \hat{k}_{3D} \cdot \vec{\sigma}$. The LL wave functions are

$$\Psi_{n, \vec{k}_{3D}, \Sigma}(\vec{r}, u) = e^{i\vec{k}_{3D} \cdot \vec{r}} \phi_n[u - u_0(k_{3D}, \Sigma)] \otimes \chi_{\Sigma}(\vec{k}_{3D}), \quad (7)$$

where the central positions $u_0(k_{3D}, \Sigma) = \Sigma l_{so}^2 k_{3D}$; χ_{Σ} are eigenstates of 3D helicity $\hat{\Sigma}_{3D}$ with eigenvalues $\Sigma = \pm 1$.

Inside each LL, the spectra are flat with respect to \vec{k}_{3D} and Σ . This realizes the spatial separation of the 3D Weyl fermion modes as shown in Fig. 1(b). Similarly to the 3D case, after the LLL projection, we have the relation $PuP = (\vec{p} \cdot \vec{\sigma})l_{so}^2/\hbar$, and then the noncommutative relations among coordinates are

$$[r_i, u]_{LLL} = il_{so}^2 \sigma_i, [r_i, r_j]_{LLL} = 0, \quad (8)$$

for $i = x, y, z$. The 4D LLs can be viewed as states of the 6D phase space of a 3D system: increasing the width along the u direction corresponds to increasing the bulk momentum cutoff $k_{3D} < k_{3D}^B \equiv L_u/(2l_{so}^2)$. If the LLL is fully filled, the total number of states is given by $\mathcal{N} = L_x L_y L_z L_u^3 / (24\pi^2 l_{so}^6)$. Reexpressing $L_u = 2k_{3D}^B l_{so}^2$, we find $\mathcal{N} = (1/3\pi^2) L_x L_y L_z (k_{3D}^B)^3$, which is the conventional state counting of a 3D system expressed in terms of the 6D phase space volume. With an open boundary imposed along the u direction, 3D helical Weyl fermion modes appear on the boundary. Now let us consider the generalized 4D quantum Hall effects [10] as the nonlinear electromagnetic response of (4 + 1)D LL system to the external electric and magnetic (EM) fields, with $\vec{E} \parallel \vec{B}$ in the xyz space. Without loss of generality, we choose the EM fields as $\vec{E} = E\hat{z}$ and $\vec{B} = B\hat{z}$, which are minimally coupled to the spin-1/2 fermion,

$$H_{LL}^{4D}(E, B) = -\frac{\hbar^2}{2m} \nabla_u^2 + \frac{1}{2}m\omega^2(u + il_{so}^2 \vec{D} \cdot \vec{\sigma})^2, \quad (9)$$

where $\vec{D} = \vec{\nabla} - i(e/\hbar c)\vec{A}_{em}$. Here, \vec{A}_{em} is the U(1) magnetic vector potential in the Landau gauge with $A_{em,x} = 0$, $A_{em,y} = Bx$, and $A_{em,z} = -cEt$. We define $l_B = \sqrt{\hbar c/(eB)}$, where $eB > 0$ is assumed.

The \vec{B} field further reorganizes the chiral plane wave states inside the n -th 4D LL into a series of 2D magnetic LLs in the xy plane. For the moment, let us set $E_z = 0$. The eigenvalues $E_n = (n + \frac{1}{2})\hbar\omega_{so}$ remain the same as before without splitting, while the eigen-wave-functions are changed. We introduce a magnetic LL index m in the xy plane. For the case of $m = 0$, the eigen-wave-functions are spin polarized as

$$\Psi_{n,m=0}(k_y, k_z) = e^{ik_y y + ik_z z} \phi_n[u - u_0(k_z, m = 0)] \otimes \chi_{m=0}[x - x_0(k_y)], \quad (10)$$

where $x_0 = l_B^2 k_y$ and $\chi_0 = [\phi_0(x - x_0), 0]^T$ is the zero mode channel of the operator $-i\vec{D} \cdot \vec{\sigma}$ with the eigenvalue of $\lambda_0 = k_z$. The central positions of the u -direction harmonic oscillators are $u_0(k_z, m = 0) = l_{so}^2 k_z$. For $m \geq 1$, the eigenmodes of $-i\vec{D} \cdot \vec{\sigma}$ come in pairs as

$$\chi_{m,\pm}[x - x_0(k_y)] = \begin{bmatrix} \alpha_{m,\pm} \phi_m(x - x_0) \\ \beta_m \phi_{m-1}(x - x_0) \end{bmatrix}, \quad (11)$$

where coefficients $\alpha_{m,\pm} = l_B k_z \pm \sqrt{l_B^2 k_z^2 + 2m}$, $\beta_m = -i\sqrt{2m}$, and the eigenvalues are $\lambda_{m,\pm} = \pm\sqrt{k_z^2 + 2ml_B^{-2}}$. The corresponding eigen-wave-functions are $\Psi_{n,m,\pm}(k_y, k_z) = e^{ik_y y + ik_z z} \phi_n[u - u_0(k_z, m, \pm)] \chi_{m,\pm}[x - x_0(k_y)]$, where the central positions $u_0(k_z, m, \pm) = \pm l_{so}^2 \sqrt{k_z^2 + 2ml_B^{-2}}$.

For the solutions of Eq. (10) with the same 4D LL index n , the 2D magnetic LLs with index $m = 0$ are singled out. The central positions of states in this branch are linear with k_z , and thus run across the entire u axis, while those of other branches with $m \geq 1$ only lie in one half of the space as shown in Fig. 2. After turning on E_z , k_z is accelerated with time as $k_z(t) = k_z(0) + eE_z t/\hbar$, and thus, the central positions $u_0(m = 0, k_z)$ moves along the u axis. Only the $m = 0$ branch of the magnetic LL states contribute to the charge pumping which results in an electric current along the u direction. Within the time interval Δt , the number of states with each filled 4D LL passing a cross section perpendicular to the u axis is $N = (L_x L_y / (2\pi l_B^2)) (eE \Delta t L_z / (2\pi))$, which results in the electric current density $(e / (L_x L_y L_z)) (dN / dt)$. If the number of fully filled 4D LLs is n_{occ} , the total current density along the u axis is

$$j_u = n_{occ} \alpha \frac{e}{4\pi^2 \hbar} \vec{E} \cdot \vec{B}, \quad (12)$$

where $\alpha = e^2 / (\hbar c)$ is the fine-structure constant. This quantized nonlinear electromagnetic response is in agreement with results from the effective theory [10] as the 4D generalization of the QH effect. If we impose open boundary conditions perpendicular to the u direction, the above charge pump process corresponds to the chiral anomalies of Weyl fermions with opposite chiralities on the two 3D boundaries, respectively. Since they are spatially separated, the chiral current corresponds to the electric current along the u direction.

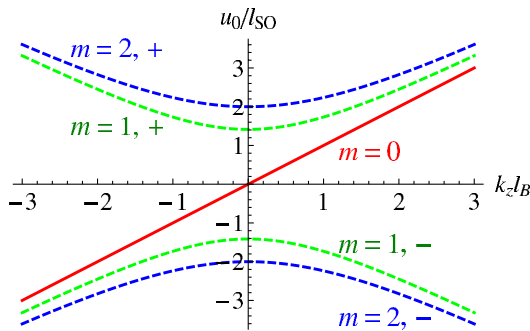


FIG. 2 (color online). The central positions $u_0(m, k_z, \nu)$ of the 4D LLs in the presence of the magnetic field $\vec{B} = B\hat{z}$. Only the branch of $m = 0$ [shown by the red (solid) line] runs across the entire u axis, which gives rise to quantized charge transport along u axis in the presence of $\vec{E} \parallel \vec{B}$ as indicated in Eq. (12). This plot takes parameters $l_{so} = l_B$.

Although the density of states of our 4D LL systems is different from the 4D TIs in the lattice system with translational symmetry [10], their electromagnetic responses obey the same Eq. (12). It is because that only the spin-polarized $m = 0$ branch of LLs, $\Psi_{n,m=0}(k_y, k_z)$, is responsible for the charge pumping. For this branch, B_z field quantizes the motion in the xy plane so that the x and u coordinates play the role of k_y and k_z , respectively. Consequently, the system can be viewed as the 4D phase space of coordinates y and z , and scales uniformly as $L_x L_y L_z L_u$ with the conventional thermodynamic limit of a 4D system.

The 3D LL Hamiltonian Eq. (1) can be realized in strained semiconductors by generalizing the method in Ref. [13] from 2D to 3D. For semiconductors with the zinc-blende structure, the t_{2g} components of the strain tensor generate SO coupling as

$$H_{stm} = -\lambda \{ \epsilon_{xy} (p_x \sigma_y - p_y \sigma_x) + \epsilon_{yz} (p_y \sigma_z - p_z \sigma_y) + \epsilon_{zx} (p_z \sigma_x - p_x \sigma_z) \}, \quad (13)$$

where $\lambda = 4 \times 10^5$ m/s and 9×10^5 m/s for GaAs and InSb, respectively [38]. The z -dependent Rashba SO coupling is induced by the strain component ϵ_{xy} , which can be generated by applying the pressure along the [110] direction without inducing ϵ_{yz} and ϵ_{zx} [13,39]. Furthermore, if the pressure linearly varies along the z axis, such that $\epsilon_{xy} = gz$ where g is the strain gradient, then we arrive at the SO coupling in Eq. (1) with the relation $\omega_{so} = g\lambda$. A strain gradient of 1% over the length of $1 \mu\text{m}$ leads to the LL gap $\hbar\omega = 2.6 \mu\text{eV}$ in GaAs. It corresponds to the temperature of 30 mK, which is accessible within the current low temperature technique. The strain gradient at a similar order has been achieved experimentally [13,40]. The harmonic potential in Eq. (1) is equivalent to a standard parabolic quantum well along the z axis [41], which is constructed by an alternating growth of GaAs and $\text{Al}_x\text{Ga}_{1-x}\text{As}$ layers. The harmonic frequency can be controlled by varying the thickness of different layers.

In conclusion, we have generalized LLs to 3D and 4D in the Landau-like gauge by coupling spatially dependent SO couplings with harmonic potentials. This method can be generalized to arbitrary dimensions by replacing the Pauli matrices with the Γ matrices in corresponding dimensions. These high dimensional LLs exhibit spatial separation of helical or chiral fermion modes with opposite helicities, which give rise to gapless helical or chiral boundary modes. The 4D LLs give rise to the quantized nonlinear electromagnetic responses as a spatially separated (3 + 1)D chiral anomaly. Many interesting open problems are left for future studies. For example, in the Supplemental Material [37], we present a preliminary effort on constructing of Laughlin wave functions in 4D LLs with spin polarizations. The generalizations of LLs to 3D and 4D Dirac fermions are also given there. A full study of the interaction effects on the high dimensional fractional

topological states based on LLs will be investigated in future publications.

Y.L. and C.W. thank J. Hirsch, N. P. Ong, L. Sham, and Z. Wang and Y.S. Wu for helpful discussions. Y.L. and C.W. are supported by the NSF DMR-1105945 and AFOSR FA9550-11-1-0067(YIP), and S.-C.Z. is supported by the NSF under Grant No. DMR-1305677. C.W. also acknowledges the support from the NSF of China under Grant No. 11328403. Y.L. thanks the Inamori Fellowship and the support at the Princeton Center for Theoretical Science.

-
- [1] X.-L. Qi and S.-C. Zhang, *Phys. Today* **63**, 33 (2010).
- [2] X.-L. Qi and S.-C. Zhang, *Rev. Mod. Phys.* **83**, 1057 (2011).
- [3] M. Z. Hasan and C. L. Kane, *Rev. Mod. Phys.* **82**, 3045 (2010).
- [4] K. Klitzing, G. Dorda, and M. Pepper, *Phys. Rev. Lett.* **45**, 494 (1980).
- [5] D. J. Thouless, M. Kohmoto, M. P. Nightingale, and M. den Nijs, *Phys. Rev. Lett.* **49**, 405 (1982).
- [6] B. I. Halperin, *Phys. Rev. B* **25**, 2185 (1982).
- [7] M. Kohmoto, *Ann. Phys. (N.Y.)* **160**, 343 (1985).
- [8] F. D. M. Haldane, *Phys. Rev. Lett.* **61**, 2015 (1988).
- [9] S. Zhang and J. Hu, *Science* **294**, 823 (2001).
- [10] X.-L. Qi, T. L. Hughes, and S.-C. Zhang, *Phys. Rev. B* **78**, 195424 (2008).
- [11] C. L. Kane and E. J. Mele, *Phys. Rev. Lett.* **95**, 226801 (2005).
- [12] B. A. Bernevig and S. C. Zhang, *Phys. Rev. Lett.* **96**, 106802 (2006).
- [13] B. A. Bernevig, T. L. Hughes, and S. C. Zhang, *Science* **314**, 1757 (2006).
- [14] L. Fu and C. L. Kane, *Phys. Rev. B* **76**, 045302 (2007).
- [15] J. E. Moore and L. Balents, *Phys. Rev. B* **75**, 121306 (2007).
- [16] R. Roy, *New J. Phys.* **12**, 065009 (2010).
- [17] M. König, S. Wiedmann, C. Brune, A. Roth, H. Buhmann, L. W. Molenkamp, X.-L. Qi, and S.-C. Zhang, *Science* **318**, 766 (2007).
- [18] D. Hsieh, D. Qian, L. Wray, Y. Xia, Y. S. Hor, R. J. Cava, and M. Z. Hasan, *Nature (London)* **452**, 970 (2008).
- [19] H. Zhang, C.-X. Liu, X.-L. Qi, X. Dai, Z. Fang, and S.-C. Zhang, *Nat. Phys.* **5**, 438 (2009).
- [20] Y. Xia *et al.*, *Nat. Phys.* **5**, 398 (2009).
- [21] Y. L. Chen *et al.*, *Science* **325**, 178 (2009).
- [22] X.-L. Qi, T. L. Hughes, S. Raghu, and S.-C. Zhang, *Phys. Rev. Lett.* **102**, 187001 (2009).
- [23] A. Kitaev, *AIP Conf. Proc.* **1134**, 22 (2009).
- [24] S. Ryu, A. Schnyder, A. Furusaki, and A. Ludwig, *New J. Phys.* **12**, 065010 (2010).
- [25] D. Karabali and V. Nair, *Nucl. Phys.* **B641**, 533 (2002).
- [26] H. Elvang and J. Polchinski, *C. R. Acad. Sci. Paris Ser. IV* **4**, 405 (2003).
- [27] B. A. Bernevig, J. Hu, N. Toumbas, and S. C. Zhang, *Phys. Rev. Lett.* **91**, 236803 (2003).
- [28] K. Hasebe, *SIGMA* **6**, 071 (2010).
- [29] J. M. Edge, J. Tworzydło, and C. W. J. Beenakker, *Phys. Rev. Lett.* **109**, 135701 (2012).
- [30] Y. Li and C. Wu, *Phys. Rev. Lett.* **110**, 216802 (2013).
- [31] Y. Li, K. Intriligator, Y. Yu, and C. Wu, *Phys. Rev. B* **85**, 085132 (2012).
- [32] Y. Li, X. Zhou, and C. Wu, *Phys. Rev. B* **85**, 125122 (2012).
- [33] E. Tang, J.-W. Mei, and X.-G. Wen, *Phys. Rev. Lett.* **106**, 236802 (2011).
- [34] K. Sun, Z. Gu, H. Katsura, and S. Das Sarma, *Phys. Rev. Lett.* **106**, 236803 (2011).
- [35] T. Neupert, L. Santos, C. Chamon, and C. Mudry, *Phys. Rev. Lett.* **106**, 236804 (2011).
- [36] J. E. Hirsch (private communication); *J. Supercond.* **26**, 2239 (2013).
- [37] See Supplemental Material at <http://link.aps.org/supplemental/10.1103/PhysRevLett.111.186803> for discussions on classical equations of motion, mismatched trap and spin-orbit frequencies, delocalized helical modes, Laughlin-type wave functions, and high dimensional LLs of Dirac electrons.
- [38] R. Ranvaud, H.-R. Trebin, U. Rössler, and F. H. Pollak, *Phys. Rev. B* **20**, 701 (1979).
- [39] G. Pikus and A. Titkov, *Spin Relaxation under Optical Orientation in Semiconductors*, Modern Problems in Condensed Matter Sciences Vol. 8, Chap. 3 (North-Holland, Amsterdam, 1984), p. 73.
- [40] Q. Shen and S. Kycia, *Phys. Rev. B* **55**, 15791 (1997).
- [41] R. C. Miller, A. C. Gossard, D. A. Kleinman, and O. Munteanu, *Phys. Rev. B* **29**, 3740 (1984).